Strojnícky časopis – *Journal of* MECHANICAL ENGINEERING,
VOL 75 (2025), NO 2, 39 – 52

ACCURACY ANALYSIS OF THE TURBULENCE MODELS K–Ω GEKO AND RSM STRESS-BSL USING THE EXAMPLE OF A 2D HILL FLOW PROBLEM

MURODIL Madaliev[1], AYBEK Arifjanov[2], LUKMON Samiev[2], ZOKHIDJON Abdulkhaev[1*]

[1]*Fergana State Technical University, Fergana, Uzbekistan, e – mail: zokhidjon@fstu.uz*
[2]*National Research University "Tashkent Institute of Irrigation and Agricultural Mechanization Engineers institute", Tashkent, Uzbekistan*

Abstract: This paper presents a numerical simulation of a two-dimensional turbulent flow around a hill (2D Hill Flow) corresponding to the ERCOFTAC Case 018 reference case. Two turbulence models were used to calculate the turbulent flow: a modified two-parameter k–ω GEKO model and a Reynolds stress model RSM Stress-BSL. Numerical calculations were performed in the ANSYS Fluent software environment using an identical computational grid and boundary conditions reproducing the conditions of experimental measurements. A comparison of the obtained velocity profiles and Reynolds stress tensor components with reference experimental data was carried out. Based on the comparison, an analysis of the accuracy and adequacy of both turbulence models in describing a complex flow structure, including the separation and recirculation zones, was performed.

KEYWORDS: Navier–Stokes equations, SST model,RSM Reynolds stress model, ANSYS.

1 Introduction

Modeling turbulent flows around complex geometries such as hills, ridges, stepped obstacles and other streamlined bodies is one of the most challenging and urgent problems of modern computational fluid dynamics (CFD). These types of flows are characterized by high velocity and pressure gradients, flow separation, vortex structures and reverse flow zones, which requires the use of accurate and reliable turbulence models. The analysis of such flows has important practical application in a wide range of engineering disciplines: from aerodynamics and aerospace engineering to hydraulic structures, ventilation systems, pipelines and streamlining of infrastructure elements such as bridges, buildings and vehicles. In particular, when flowing around elevated elements such as airfoils, humps or hills, complex separation and recirculation zones are formed, the accurate prediction of which is critical for estimating drag, heat transfer, aerodynamic loads and noise characteristics. Errors in modeling these phenomena can lead to significant calculation errors, and consequently to the inefficiency of the design and a violation of its reliability [1–7]. Therefore, the development and validation of numerical methods capable of accurately describing the behavior of turbulent flow near such complex geometries remain a priority task for researchers and engineers. Particularly relevant is the use of reference test cases, such as 2D Hill Flow, which allow comparing the results of various models with experimental data and clarifying the areas of their applicability. One of the widely used test cases for validating numerical models is the 2D Hill Flow problem proposed within the ERCOFTAC (European Research Community on Flow, Turbulence and Combustion) database. This benchmark case, known as Case 018, has been studied in detail both experimentally and numerically in a number of studies, including [8–10] and numerous subsequent publications aimed at testing turbulent models of varying complexity.

DOI: 10.2478/scjme-2025-0022, Print ISSN 0039-2472, On-line ISSN 2450-5471

For the numerical description of turbulent flows, the most widely used models today are those based on the averaged Reynolds Navier–Stokes equations (RANS), which allow to significantly reduce computational costs compared to more detailed methods such as LES (Large Eddy Simulation) or DNS (Direct Numerical Simulation). Among the large number of RANS models, special attention is paid to two approaches with different levels of complexity and accuracy: the modified k–ω GEKO (Generalized k–omega) model and the Reynolds Stress Model (RSM) in the Stress-BSL version. The k–ω GEKO model was developed by Ansys as a generalized version of the traditional k–ω model with the ability to adapt to various types of flows by changing the coefficients in the equations. Its advantage is its versatility and increased accuracy compared to classical two-parameter models in a wide range of problems, including internal and external flows, turbulent jets, and diffusers. On the other hand, the RSM Stress-BSL model is a more advanced approach that directly solves the transport equations for the Reynolds stress tensor components. This allows taking into account turbulence anisotropy, streamline curvature, rotation effects, and secondary vortex interactions, making it particularly suitable for flows with strong recirculation, flow separation, and complex geometry. However, high accuracy is accompanied by increased computational cost and complexity in setting up boundary conditions [11–15]. Despite the widespread use of k–ε and k–ω models in engineering practice, numerous studies show that under conditions of highly developed recirculation and in the presence of complex turbulent structures, they can give noticeable deviations from experimental data. It is in such cases that it is advisable to use more complex models, such as RSM, which provide a better match to real flows. In this paper, a detailed comparison of the efficiency of the k–ω GEKO and RSM Stress-BSL models is carried out in the numerical solution of the reference problem of flow past a two-dimensional hill (ERCOFTAC Hill Flow Case 018) [16–19]. Particular attention is paid to comparing the numerical results with experimental data on velocity profiles, pressure distributions and other flow characteristics, in order to determine the model that provides the greatest accuracy under the given conditions.

2 Physical and mathematical formulation of the problem

In this paper, we consider a two-dimensional turbulent incompressible fluid flow over a single polynomially shaped hill installed on the lower wall of a rectangular channel. This case (Case A from the ERCOFTAC Case 018 database) is a benchmark problem with developed recirculation and flow separation zones, which makes it suitable for assessing the accuracy of RANS-class turbulence models. The geometric configuration and the computational grid (of 88,500 cells) are shown in Fig. 1. The channel height is H = 170 mm, and the maximum height of the hill is h_{max} = 28 mm. The origin is located at the top of the hill, with a symmetrical setting along the x-axis. The simulation domain extends from x = -1500 mm to x = 800 mm, covering the inlet zone, the hill itself, and a sufficiently long outlet zone for complete flow stabilization after recirculation. The working fluid is water with a kinematic viscosity of $\nu = 1 \times 10^{-6}$ m²/s. The average velocity at the inlet axis of symmetry is U_0 = 2.147 m/s, which corresponds to the Reynolds number for the height of the hill: $Re = (U_0 \times h_{max}) / \nu \approx 60{,}000$.

3 Mathematical model

For numerical simulation of the channel flow, the Reynolds-based averaged Navier–Stokes (RANS) system of equations was used. These equations serve as a basis for describing the motion of an incompressible viscous fluid and allow modeling complex turbulent flows by separating the quantities into average and pulsation components. Reynolds averaging allows reducing the problem to solving a system of equations for average values of velocity and pressure, while the effect of turbulent pulsations is taken into account by adding additional terms - Reynolds stresses. This approach provides a compromise between the accuracy of modeling and acceptable costs of computing resources, making it widely applicable in engineering practice. The RANS system of equations includes a continuity equation expressing the law of conservation of mass, and averaged momentum equations describing the change in velocity components under the action of pressure gradients, viscous forces and turbulent stresses [20–25]. To close the system of equations, it is necessary to use a turbulence model that allows determining the values of Reynolds stresses based on the average flow parameters.

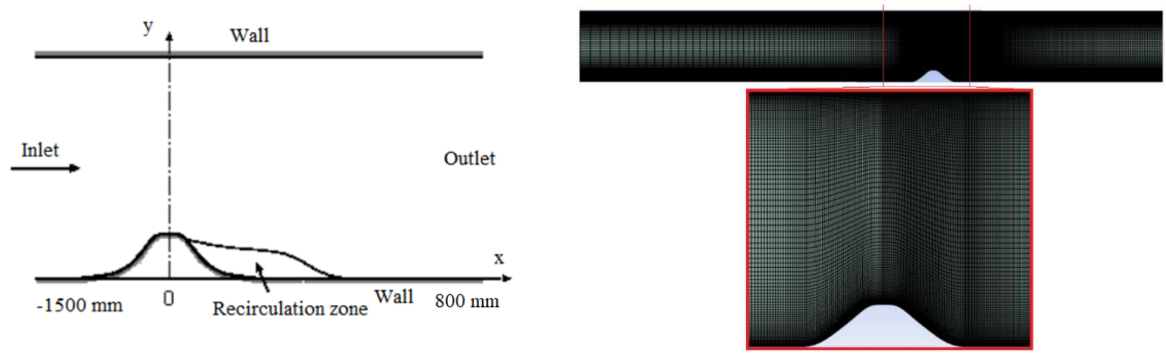

Fig. 1. Channel geometry and computational grid.

$$\frac{\partial \bar{u}_i}{\partial x_i} = 0 \tag{1}$$

The equation of conservation of momentum, which describes the change in the velocity of a fluid under the influence of external and internal forces:

$$\frac{\partial \bar{u}_i}{\partial t} + \bar{u}_j \frac{\partial \bar{u}_i}{\partial x_j} = -\frac{1}{\rho}\frac{\partial \bar{p}}{\partial x_i} + \nu \frac{\partial^2 \bar{u}_i}{\partial x_j \partial x_i} + \frac{\partial \tau_{ij}}{\partial x_i} \tag{2}$$

here

$\bar{u}_i$ - components of the average velocity field, $\bar{p}$ - average pressure, ν - kinematic viscosity, τ_{ij} - stress tensor components, ρ - density. The remaining values are presented in the works [19, 23].

4 Turbulence models

The GEKO (Generalized k-ω) SST turbulence model [26–28] is a modified version of the standard k-ω SST model designed to provide a more flexible and accurate description of turbulent flows in various regimes, including supersonic and hypersonic ones. This model was developed to eliminate the shortcomings of traditional two-parameter turbulence models and improve adaptability to various flow conditions.

$$\begin{cases} \dfrac{\partial(\rho k)}{\partial t} + \dfrac{\partial\left(\rho \bar{U}_j k\right)}{\partial x_j} = P_k - C_\mu \rho k \omega + \dfrac{\partial}{\partial x_j}\left[\left(\mu + \dfrac{\mu_t}{\sigma_k}\right)\dfrac{\partial k}{\partial x_j}\right], \\ \dfrac{\partial(\rho \omega)}{\partial t} + \dfrac{\partial\left(\rho \bar{U}_j \omega\right)}{\partial x_j} = C_{\omega 1} F_1 \dfrac{\omega}{k} P_k - C_{\omega 2} F_2 \rho \omega^2 + \rho F_3 CD + \dfrac{\partial}{\partial x_j}\left[\left(\mu + \dfrac{\mu_t}{\sigma_\omega}\right)\dfrac{\partial \omega}{\partial x_j}\right]. \end{cases} \tag{3}$$

Turbulent eddy viscosity is calculated by: $\mu_t = \rho \nu_t = \rho \dfrac{k}{\max\left(\omega, S / C_{Realize}\right)}$.

$$P_k = -\tau_{ij} \frac{\partial U_i}{\partial x_j}, \tag{4}$$

$$\tau_{ij}^{EV} = -\rho \overline{u_i^{'} u_j^{'}} = \mu_t 2 S_{ij} - \frac{2}{3} \rho k \delta_{ij}, \tag{5}$$

$$CD = \frac{2}{\sigma_\omega} \frac{1}{\omega} \frac{\partial k}{\partial x_j} \frac{\partial \omega}{\partial x_j}, \tag{6}$$

$$\tau_{ij} = \tau_{ij}^{EV} - C_{CORNER} \frac{1.2\mu_t}{\max\left(0.3\omega, \sqrt{0.5\left(S^2 + \Omega^2\right)}\right)} \left(S_{ik}\Omega_{kj} - \Omega_{ik}S_{kj}\right), \tag{7}$$

$$S_{ij} = \frac{1}{2}\left(\frac{\partial U_i}{\partial x_j} + \frac{\partial U_j}{\partial x_i}\right),\ \Omega_{ij} = \frac{1}{2}\left(\frac{\partial U_i}{\partial x_j} - \frac{\partial U_j}{\partial x_i}\right), \quad S = \sqrt{2 S_{ij} S_{ij}},\ \Omega = \sqrt{2 \Omega_{ij} \Omega_{ij}}. \tag{8}$$

The remaining coefficients and functions were presented in the article. [26].

The Reynolds Stress Model (RSM) is one of the most comprehensive approaches to the numerical description of turbulent flows within the framework of the averaged Navier–Stokes (RANS) equations. Unlike simpler two-parameter models (such as k–ε or k–ω), the RSM directly solves the transport equations for the six independent components of the Reynolds stress tensor $ui'uj'$, as well as the equation for the dissipation of turbulent energy ε. This allows for a more accurate account of turbulence anisotropy, the influence of streamline curvature, the effects of stress rotation and non-uniformity. The Stress-BSL variant is an improved version of the RSM using the Baseline Stress Limiter, proposed to increase the stability of the calculations and improve the behavior of the model in the near-surface regions. The Reynolds stress equations are as follows:

$$\frac{\partial \mathrm{R}_{ij}}{\partial t} + \bar{u}_k \frac{\partial \mathrm{R}_{ij}}{\partial x_k} = P_{ij} - \varepsilon_{ij} + D_{ij} + \Pi_{ij} + \Phi_{ij}. \tag{9}$$

Here Rij are the components of the Reynolds stress tensor, Pij is the production of turbulent stresses, ϵij is the dissipation, Dij is the diffusion, Πij is the pressure and Φij is the source of thermal stresses. The remaining values are presented in the works [28–31].

5 Method of solution

For numerical simulation of turbulent flow over a single hill, two turbulence models were used in the ANSYS Fluent software environment: the Reynolds stress model RSM Stress-BSL and the generalized k–ω GEKO model. In both cases, the Coupled scheme was used to relate pressure and velocity, which provides increased stability and convergence in the presence of complex gradients. The Least Squares Cell-Based scheme was chosen to approximate gradients, and the Second Order Upwind scheme was chosen for pressure and motion equations, which provides a more accurate resolution of flow separation and recirculation zones. In the case of the RSM model, the Reynolds stress discretization and specific dissipation equations were performed using the First Order Upwind scheme, while for the k–ω GEKO model, the equations for turbulence kinetic energy and dissipation frequency were solved using the second order scheme. The distribution of relaxation coefficients was chosen identical: 0.5 for pressure and momentum, 0.75 for turbulent parameters (Reynolds stresses, k and ω), which ensured stable convergence. The residual convergence criteria were set at the level of 1e-3 for all equations, and the convergence progress was monitored through Residual Monitors graphs. A condensed computational grid with $y^+ < 1$ allowed us to abandon wall functions and use an integrated approach to resolving the boundary layer. The use of second-order schemes and adaptive turbulence models ensured high accuracy of modeling in the region of strong gradients and vortex structures behind the hill.

6 Results and discussion

Figures 2–6 show a comparison of the flow velocity components U and V, as well as the Reynolds stresses $u'u'$, $v'v'$, $u'v'$ on the sections x=−300, 0, 30, 50, 70, 90, 134, 185, 500 mm, obtained using the k–ω GEKO and RSM Stress-BSL models, with experimental data.

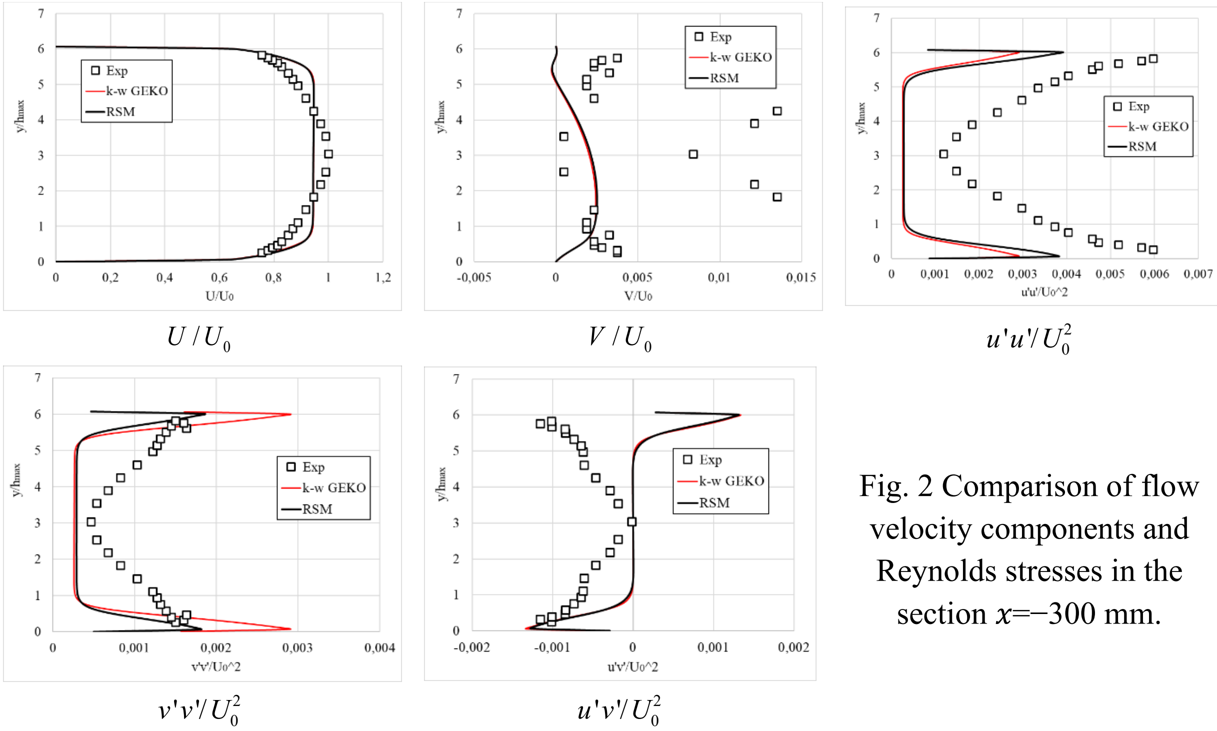

Fig. 2 Comparison of flow velocity components and Reynolds stresses in the section x=−300 mm.

Figure 2 shows the profiles of the mean velocity components and Reynolds stresses measured and calculated at the x=−300 mm cross-section along the channel height (y axis, normalized to the hill height). The graphs demonstrate the distributions of the longitudinal (U) and transverse (V) velocities, as well as the normal and tangential components of the Reynolds stresses: $u'u'$, $v'v'$, $u'v'$, reduced to dimensionless form through. The analysis shows that the RSM Stress-BSL model (red line) better reproduces the transverse velocity profile and stress anisotropy, while the k–ω GEKO model (black line) more accurately agrees with the experiment for the main velocity component U. Experimental data (marker) are taken from the ERCOFTAC Case 018 reference database. Good agreement between the models and the experiment is observed in the central part of the flow, while near the wall and in the region of sharp gradients the differences between the models become more noticeable.

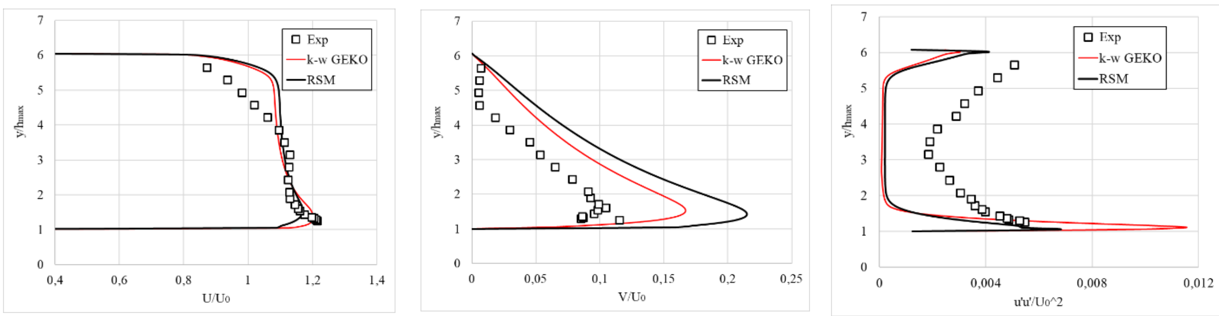

U/U_0 V/U_0 $u'u'/U_0^2$

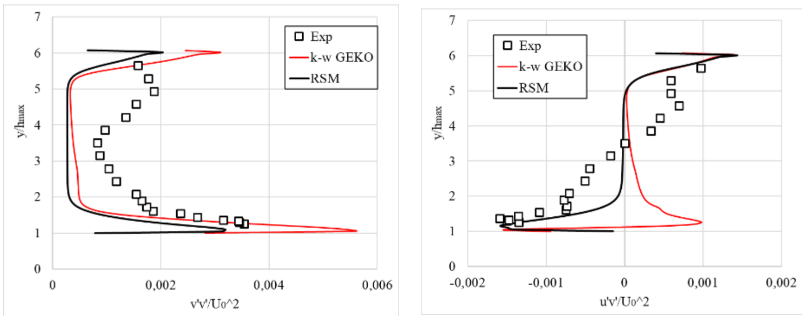

$v'v'/U_0^2$ $u'v'/U_0^2$

Fig. 3 Comparison of flow velocity components and Reynolds stresses in the cross-section x=0 mm.

Fig. 3. The vertical profiles of the dimensionless components of the mean velocity and the Reynolds stress components in the section x=0 mm - in the area of the hilltop - are presented. The graphs show that the RSM model better predicts the transverse velocity and normal components of turbulent stresses, while the GEKO model gives a smoother profile, close to the experiment for the main component of the velocity U. The greatest differences between the models are observed in the area of intense gradients and in the near-surface layers of the flow, where the effect of anisotropy is most significant. These data allow us to evaluate the accuracy and applicability of each model in the area of the hilltop, where the flow experiences strong deformations and the onset of recirculation.

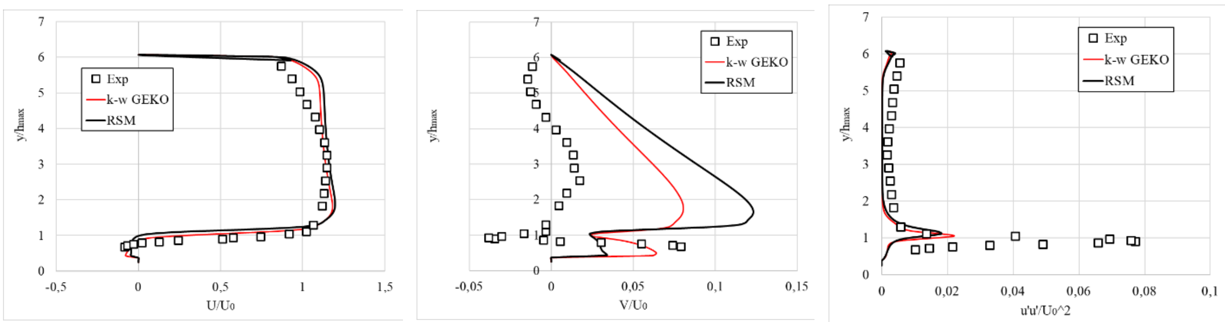

U/U_0 V/U_0 $u'u'/U_0^2$

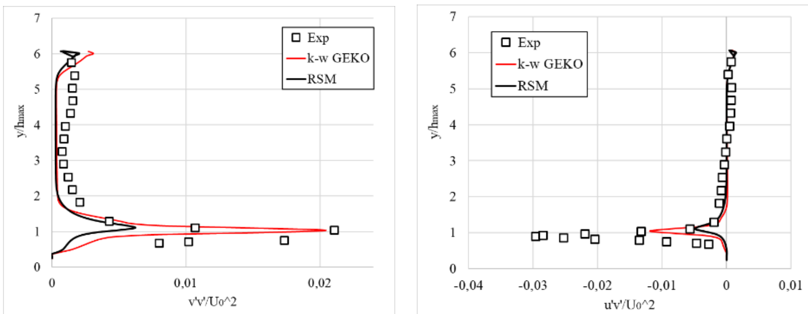

$v'v'/U_0^2$ $u'v'/U_0^2$

Fig. 4 Comparison of flow velocity components and Reynolds stresses in the cross-section x=30 mm.

In Fig. 4. in the section x=30 mm - in the area immediately after the top of the hill, where the reverse flow zone is formed. The velocity graph U clearly shows the reverse flow effect in the lower part of the channel (negative values), which is well reproduced by both models, but the RSM model demonstrates a more realistic distribution of transverse velocity and stress anisotropy. The discrepancies are especially pronounced in the tangential component, where GEKO underestimates the extreme values. This confirms the sensitivity of the results to the chosen turbulence model in the recirculation region.

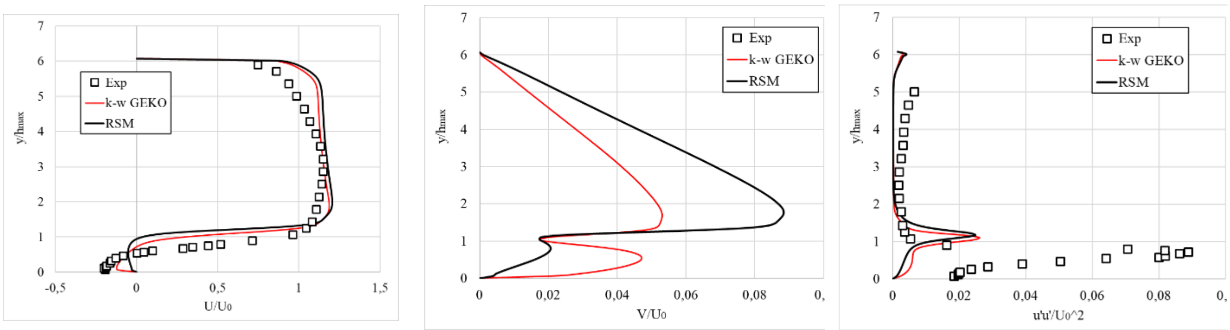

U / U_0 V / U_0 $u'u'/ U_0^2$

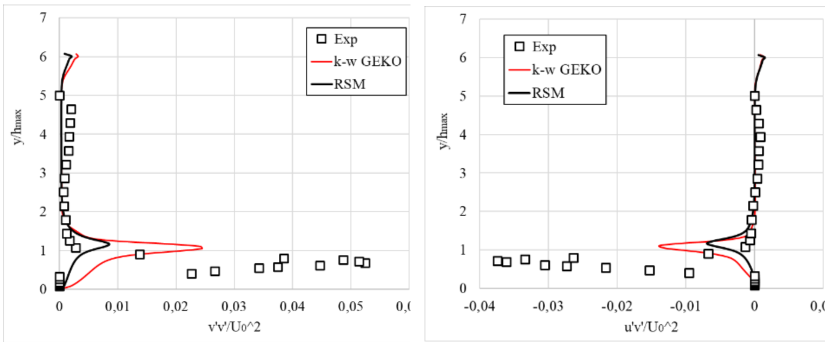

$v'v'/ U_0^2$ $u'v'/ U_0^2$

Fig. 5 Comparison of flow velocity components and Reynolds stresses in the cross-section x=50 mm.

In Fig. 5. in the section x=50 mm, the velocity profile U clearly shows a reverse flow zone in the lower part of the channel ($U/U0<0$), which is reproduced quite well by both models. However, in the distribution of the transverse velocity V, as well as in the components of the Reynolds stresses, in particular, significant discrepancies are observed between the models and the experiment. The RSM model conveys the amplitude of transverse pulsations to a greater extent, while GEKO approximately conveys trends, but underestimates extreme values. This indicates an increased sensitivity of calculations in the central separation zone and the importance of choosing a turbulence model for a correct description of the internal structure of vortices.

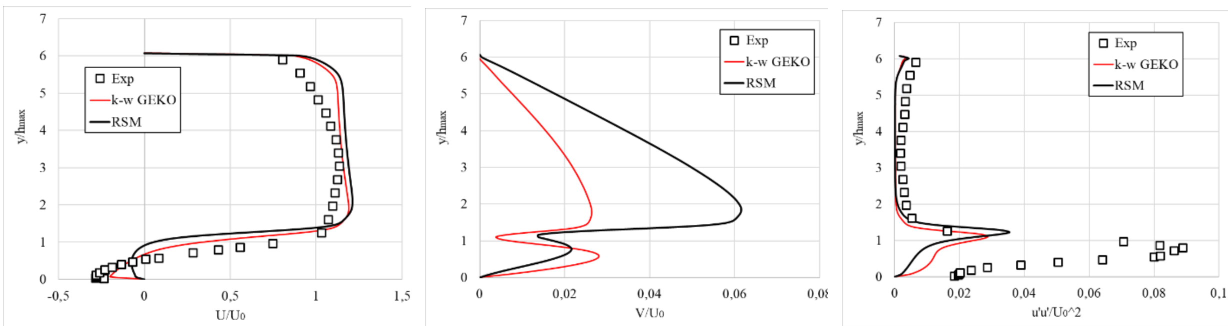

U / U_0 V / U_0 $u'u'/ U_0^2$

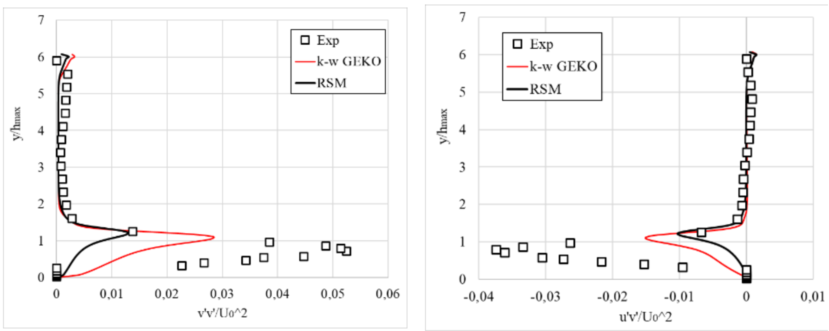

$v'v'/U_0^2$ $u'v'/U_0^2$

Fig. 6 Comparison of flow velocity components and Reynolds stresses in the cross-section x=70 mm.

From Fig. 6 it is evident that the longitudinal velocity U restores a profile close to a fully developed flow, although traces of reverse flow are still preserved in the lower part. The RSM model more accurately reproduces the shape of the transverse profile V, while GEKO shows deviations near the channel center. For the normal and tangential components of the Reynolds stresses, both models demonstrate approximate agreement with the experimental trends. This section indicates the transition of the flow to a stabilized regime with a decrease in turbulent pulsations.

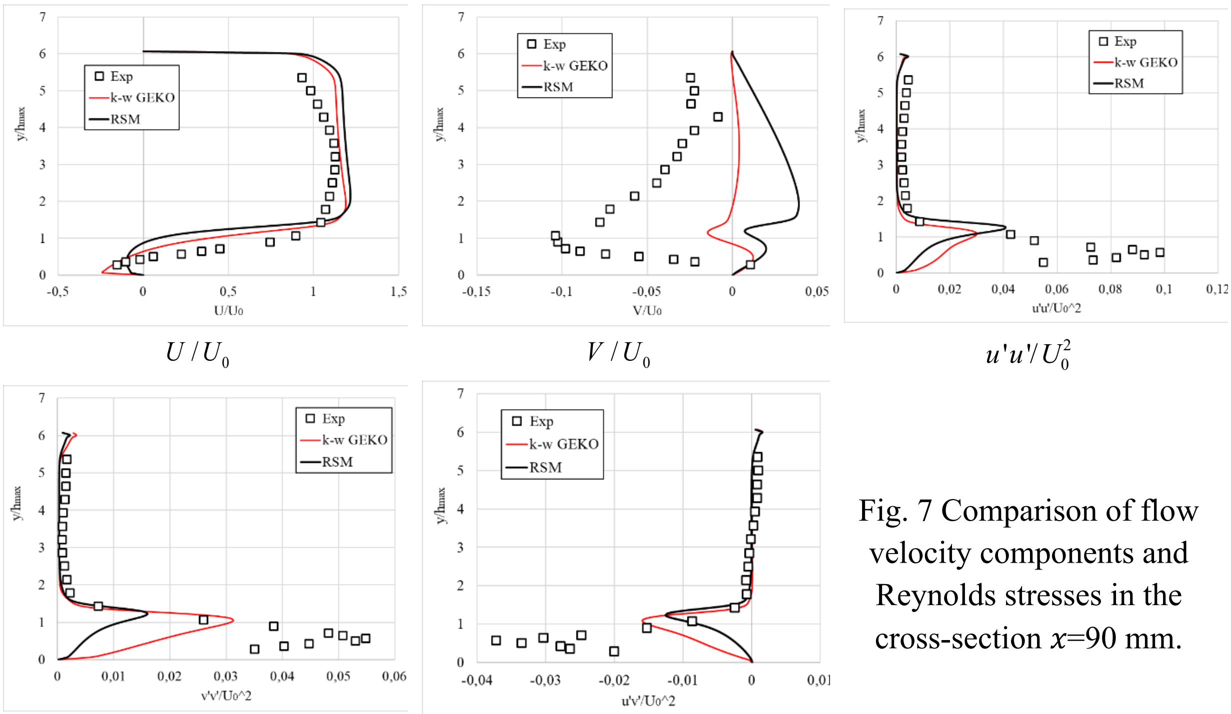

U/U_0 V/U_0 $u'u'/U_0^2$

$v'v'/U_0^2$ $u'v'/U_0^2$

Fig. 7 Comparison of flow velocity components and Reynolds stresses in the cross-section x=90 mm.

It is evident from Fig. 7 that the longitudinal velocity U completely reconstructs the profile characteristic of the applied channel flow. In the V component, both models demonstrate deviations from the experiment, with RSM slightly overestimating the transverse velocity, while GEKO gives underestimated values. The normal stress and tangential component profiles show that the RSM model better captures local maxima and anisotropic effects, especially near the wall, while GEKO smooths out the pulsations. In this region, a general attenuation of turbulent fluctuations is observed and the flow returns to a quasi-stationary regime.

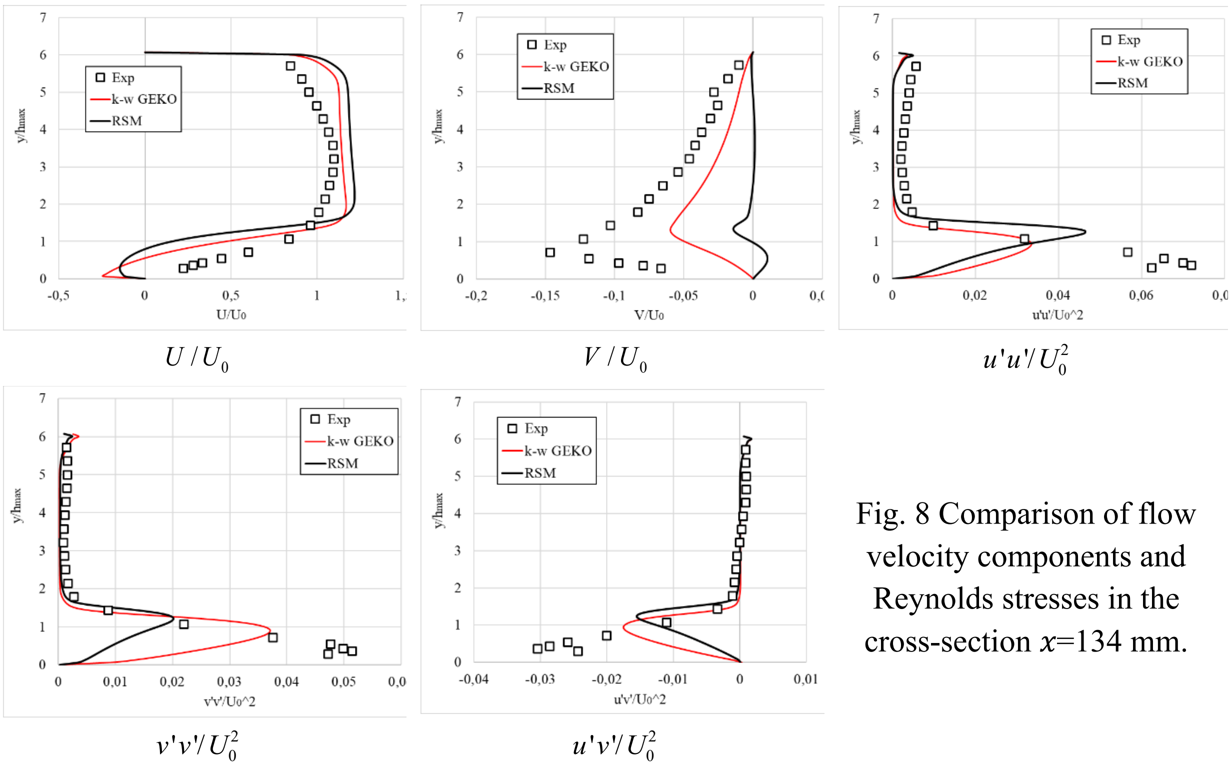

Fig. 8 Comparison of flow velocity components and Reynolds stresses in the cross-section x=134 mm.

From Fig. 8, at the section x=134 mm, located in the zone of final flow recovery after the recirculation zone. The longitudinal velocity is close to the profile of the steady-state channel flow, which is confirmed by both experimental and numerical data. However, for the transverse component, both models demonstrate noticeable discrepancies with the experiment: RSM gives a more pronounced negative shift, while GEKO approximately repeats the trend. With respect to the Reynolds stress components, it is clear that GEKO overestimates in the lower part, and RSM is closer to the wall. In general, this section demonstrates the completion of transient effects associated with separation and the restoration of symmetry and stability of the turbulent profile.

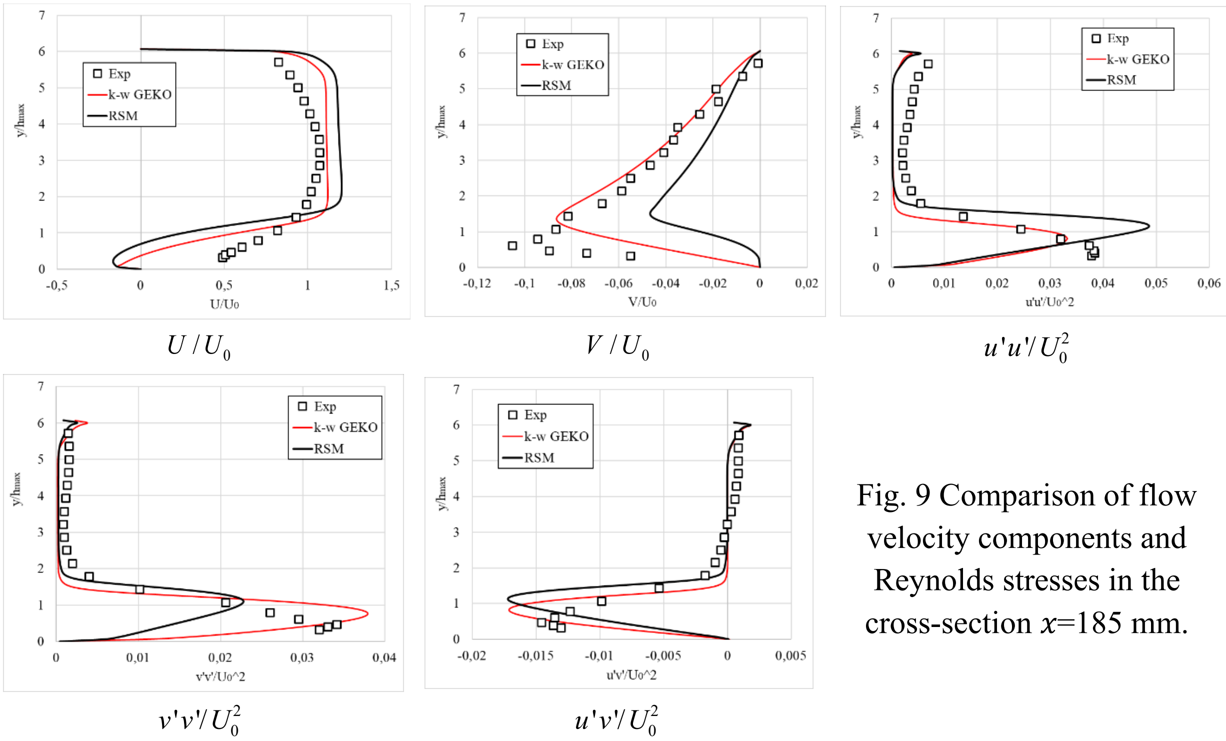

Fig. 9 Comparison of flow velocity components and Reynolds stresses in the cross-section x=185 mm.

From Fig. 9 on the section x=185 mm, located in the zone of final stabilization of the flow after the recirculation bubble. The longitudinal velocity demonstrates a complete recovery to the steady-state flow profile, although deviations indicating wake effects are still observed in the lower part. The transverse velocity indicates residual vortex motions: RSM overestimates the negative component closer to the wall, while GEKO approximately corresponds to the experiment. In the distributions of the Reynolds stress components, it is clear that both models closely convey the trends, but the accuracy of the amplitude approximation varies: GEKO overestimates in the middle part of the channel, and RSM conveys more accurately near the wall. The data confirm that after the point x≈130–150 mm, the turbulent structure of the flow is restored, but residual fluctuations persist until the end of the observation area.

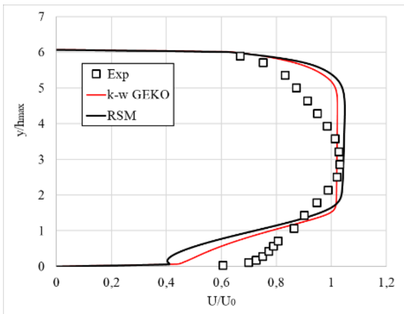

U/U_0

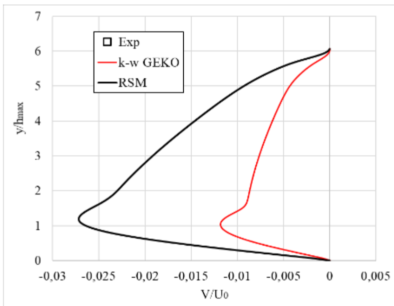

V/U_0

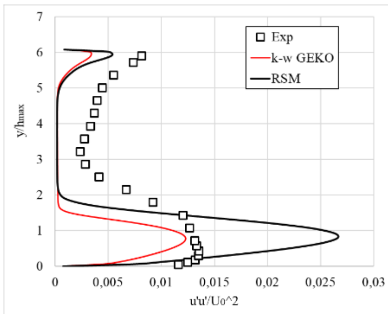

$u'u'/U_0^2$

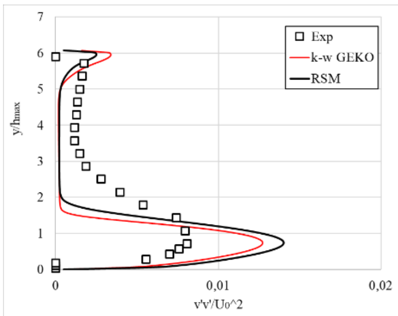

$v'v'/U_0^2$

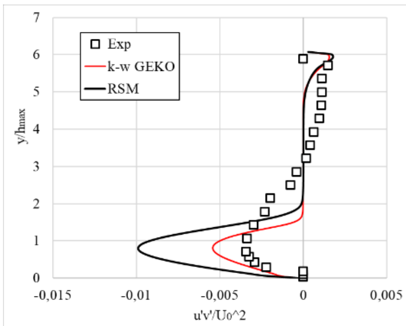

$u'v'/U_0^2$

Fig. 10 Comparison of flow velocity components and Reynolds stresses in the cross-section x=500 mm.

From Fig. 9 at the section x=500 mm - the point of the computational domain that is the farthest from the hill. In this region, the flow shows signs of final stabilization: the profile corresponds to a classical symmetrical channel flow, which is well reproduced by both models. However, the component and all three components of the Reynolds stresses still show differences from the experiment, especially near the center of the channel, where the models demonstrate different levels of turbulent activity. GEKO is closer to the experiment in the tangential component, while RSM continues to overestimate the pulsation intensity in the central zone. These observations indicate that even at a significant distance from the hill, the influence of the initial separation and vortex structures continues to affect the flow structure.

The k–ω GEKO model shows reliable and stable results in all zones, especially where the flow approaches a steady state. RSM Stress-BSL is superior in describing recirculation, anisotropic fluctuations, and turbulent stress details, but is computationally more expensive and mesh sensitive. For applications where accurate reproduction of turbulent structure is key, the RSM model is preferred, while GEKO is suitable for engineering calculations with acceptable accuracy.

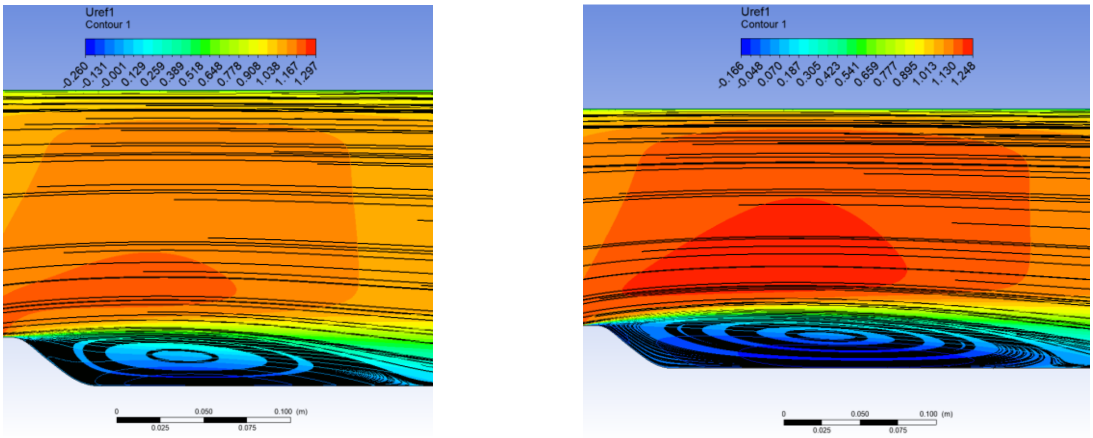

k-w GEKO RSM

Fig. 11 Comparison of velocity fields and streamlines obtained using turbulence models

Fig. 11. Comparison of the velocity fields and streamlines obtained using the k–ω GEKO (left) and RSM Stress-BSL (right) turbulence models. The color scale shows the distribution of the longitudinal velocity component in the region above the hill, and the black lines indicate the current lines visualizing the general flow structure. In both cases, the separation zone behind the hill with a characteristic recirculation bubble is clearly visible. However, the RSM model predicts a more extended reverse flow zone with a more intense vortex core and a more pronounced swirling structure of the streamlines, which corresponds to the physics of highly turbulent separation, while GEKO gives a more compact recirculation zone with less pronounced inertia and a smoothed velocity distribution, characteristic of an averaged description of the flow. This comparative analysis clearly demonstrates the difference in predicting complex flows between the universal two-parameter model (GEKO) and the full Reynolds stress model (RSM), especially in regions with large pressure gradient and intense turbulent mixing.

CONCLUSION

In this paper, we perform a comparative numerical simulation of turbulent flow past a two-dimensional hill (case A, ERCOFTAC Case 018) using the *k–ω* GEKO and RSM Stress-BSL turbulence models in the ANSYS Fluent software environment. The main focus is on assessing the ability of the models to reproduce key flow characteristics, such as velocity profiles, Reynolds stress components, and the structure of the separation and recirculation zones behind the hill. The analysis showed that the *k–ω* GEKO model demonstrates stable convergence and good agreement with experimental data outside the separation zone, especially in the stationary part of the flow. The RSM Stress-BSL model, in turn, provides a more accurate reproduction of the complex turbulent structure in the recirculation bubble region, including stress anisotropy, transverse velocities, and an extended separation zone. However, this is achieved at the expense of significantly higher computational cost and sensitivity to the quality of the computational grid. Comparison with reference experimental data showed that for engineering problems requiring fast evaluation with acceptable accuracy, the GEKO model is an effective tool. At the same time, when modeling flows with complex vortex structure, such as separations, reverse flows and strong turbulence anisotropy, it is preferable to use the RSM model, despite its computational complexity. The obtained results emphasize the importance of a reasonable choice of a turbulent model depending on the characteristics of the studied flow and the purposes of modeling. Further studies can be aimed at validating the models under changing geometries, unsteady effects or using hybrid methods (DES, LES) to improve the accuracy and physical reliability of calculations.

REFERENCES

[1] van Druenen, T., Blocken, B. "CFD simulations of cyclist aerodynamics: Impact of computational parameters", Journal of Wind Engineering and Industrial Aerodynamics 249, 105714, **2024**.

[2] Santironnarong, S., Juntasaro, E. "Behavior of Generalized K-Omega (GEKO) Parameter on Performance Prediction of Airfoils Operating in Incompressible Region", **2024**. [online] Available at: https://www.dti.or.th/page_bx.php?lang=eng&cid=326&cno=7696

[3] Mosele, J. P. G., Gross, A., Slater, J. W. "Numerical Investigation of Flow Over", Periodic Hill. In AIAA Aviation 2022 Forum (p. 3228), **2022**.

[4] Strokach, E., Borovik, I., & Haidn, O. "Simulation of the GOx/GCH4 multi-element combustor including the effects of radiation and algebraic variable turbulent prandtl approaches", Energies 13(19), 5009, **2020**.

[5] Kutiš, V., et al. "CFD Analysis of Downcomer of Nuclear Reactor VVER 440", Strojnícky časopis – Journal of Mechanical Engineering 66 (2), pp. 55 – 62, **2016**. DOI: 10.1515/scjme-2016-0018

[6] Kutiš, V., et al. "CFD Analysis of Dry Cask Nuclear Fuel Storage", Strojnícky časopis - Journal of Mechanical Engineering 69 (3), pp. 75 – 80, **2019**. DOI: 10.2478/scjme-2019-0032

[7] Lolov, D. "Dynamic Stability of A Single Walled Carbon Nanotube, Embedded in A Polymer Matrix and Conveying A Pulsatile Flow", Strojnícky časopis – Journal of Mechanical Engineering 75 (1), pp. 87 – 94, **2025**. DOI: 10.2478/scjme-2025-0009

[8] Mellen, C. P., Fröhlich, J., Rodi, W. "Lessons from direct numerical simulation and large eddy simulation for Reynolds-averaged Navier–Stokes modelling of wall-bounded flows", Journal of Fluid Mechanics, 1–35, **2000**. DOI: 10.1017/S002211200000217X

[9] Temmerman, L., Leschziner, M. A., Mellen, C. P., Fröhlich, J. "Investigation of wall-function approximations and Reynolds-stress modeling in the prediction of separated flow in a curved duct", International Journal of Heat and Fluid Flow 24(2), pp. 157 – 168, **2003**. DOI: 10.1016/S0142-727X(02)00207-7

[10] Hussein, H. J., Martinuzzi, R. J. "Energy balance for turbulent flow around a surface mounted cube placed in a channel", Physics of Fluids 8(3), pp. 764 – 780, **1996**. DOI: 10.1063/1.868850

[11] Ganatra, K. A., Chattopadhyay, H., Mathur, A. "Investigation of free and impinging jets using generalized k–ω (GEKO) turbulence model", International Journal of Heat and Fluid Flow 111, 109660, **2025**.

[12] Strokach, E., Borovik, I., Chen, F. "Numerical simulation of reacting flow in the combustion chamber and study of the impact of turbulent diffusion coefficients", Advances in Mechanical Engineering, 12(9), 1687814020954974, **2020**.

[13] Rossano, V., De Stefano, G. "Testing a generalized two-equation turbulence model for computational aerodynamics of a mid-range aircraft", Applied Sciences 13 (20), 11243, **2023**.

[14] Murodil, Madaliev, et al. "Numerical Study of Three-Phase Liquid-Gas-Solid Flow in Single and Group Hydrocyclones", Strojnícky časopis – Journal of Mechanical Engineering 75 (1), pp. 103 – 110, **2025**. DOI: 10.2478/scjme-2025-0011

[15] Pacoň, L., et al. "Prediction of Pulsating Turbine Operation Using 1-D - 3-D Co-Simulation", Strojnícky časopis – Journal of Mechanical Engineering 72 (3), pp. 81 – 96, **2022**. DOI: 10.2478/scjme-2022-0043

[16] Almeida, G. P., Durao, D. F. G., Heitor, M. V. "Wake flows behind two dimensional model hills", Exp. Thermal and Fluid Science 7, p. 87, **1992**.

[17] Almeida, G.P., Durao, D.F.G., Simoes, J.P., Heitor, M.V. "Laser-Doppler measurements of fully developed turbulent channel flow", Proc. 5th Symp. Appl Laser Techniques to Fluid Mech., pp. 5 – 12, **1990**.

[18] Hunt, J.C.R., Snyder, W.H. "Experiments on stably and neutrally stratified flow over a model three-dimensional hill", J. Fluid Mech. 96, pp. 671 – 704, **1980**.

[19] Castro, J.P., Haque, A. "The structure of a turbulent shear layer bounding a separation region", J. Fluid Mech. 179, pp. 439 – 468, **1987**.

[20] Malikov, Z. M., Nazarov, F. K. "Study of turbulence models for calculating a strongly swirling flow in an abrupt expanding channel", Computer research and modeling 13 (4), pp. 793 – 805, **2021**.

[21] Madaliev, M., Usmonov, M., Kadyrov, K., Abdullajonov, N., Mavlonova, D., Otakhanova, Z., Muminov, K. "Numerical analysis of single SC-50-800 and SC-50-500x2-x4 group centrifugal cyclones: efficiency comparison", In E3S Web of Conferences (Vol. 508, p. 06005). EDP Sciences, **2024**.

[22] Malikov, Z. M., Madaliev, M. E. "Mathematical modeling of a turbulent flow in a centrifugal separator", Vestnik Tomskogo Gosudarstvennogo Universiteta. Matematika i Mekhanika 71, pp. 121 – 138, **2021**.

[23] Li, Z., Liu, Y., Zhou, W., Wen, X., Liu, Y. "Thermal pollution level reduction by sweeping jet-based enhanced heat dissipation: A numerical study with calibrated Generalized k-ω (GEKO) model", Applied Thermal Engineering 204, 117990, **2022**.

[24] Nilufar, K. "Numerical Simulation of Aerodynamic Flow Around a Building Using OpenFOAM Software", Journal of Construction and Engineering Technology 3(2), pp. 8 – 14, **2025**. DOI: 10.24412/2181-4473-2025.3.202

[25] Utbosarov, S., Muminov, O. "Analysis of CFD Modeling of the Karkidon Reservoir Spillway Operation Using the SST Turbulent Model", Journal of Construction and Engineering Technology 3(1), pp. 1 – 15, **2025**. DOI: 10.24412/2181-4473-2025.3.101

[26] ANSYS Inc. (**2024**). "Generalized k-ω (GEKO) Two-Equation Turbulence Modeling in Ansys CFD". [online] Available at: https://www.ansys.com/resource-center/technical-paper/best-practice-geko-turbulence-modeling-in-ansys-cfd

[27] Menter, F. R. "Two-equation eddy-viscosity turbulence models for engineering applications", AIAA Journal 32 (8), pp. 1598 – 1605, **1994**.

[28] Eisfeld, B., Rumsey, C., Togiti, V. "Erratum: Verification and Validation of a Second-Moment-Closure Model," AIAA Journal 54 (9), p. 2926, **2016**. DOI: 10.2514/1.J055336

[29] Cecora, R.-D., Radespiel, R., Eisfeld, B., Probst, A. "Differential Reynolds-Stress Modeling for Aeronautics", AIAA Journal 53 (3), pp. 739 – 755, **2015**. DOI: 10.2514/1.J053250

[30] Cecora, R.-D., Eisfeld, B., Probst, A., Crippa, S., Radespiel, R. "Differential Reynolds Stress Modeling for Aeronautics", AIAA Paper 2012 – 0465, **2012**. DOI: 10.2514/6.2012-465

[31] Eisfeld, B. "Implementation of Reynolds Stress Models into the DLR-FLOWer Code", Institutsbericht, DLR-IB 124-2004/31, Report of the Institute of Aerodynamics and Flow Technology, Braunschweig, ISSN 1614-7790, **2004**.